Research on Chemical Intermediates
https://doi.org/10.1007/s11164-018-3609-4

Spectrochemical and theoretical approaches for acylhydrazone-based fluoride sensors

Jemini Jose, et al. *[full author details at the end of the article]*

Received: 6 July 2018 / Accepted: 24 September 2018

Abstract

Acylhydrazone derivatives *N*′-[1-(2-fluorophenyl)ethylidene]pyridine-3-carbohydrazide (**R1**) and *N*′-[2-fluorobenzylidene]benzohydrazide (**R2**) were synthesized from their corresponding hydrazides and characterized by spectroscopic methods. The response of these acylhydrazones towards different anions was studied by colorimetric and spectrofluorometric methods in acetonitrile. The receptors exhibited a specific response towards fluoride ion. The binding affinity of the receptors with fluoride anion was studied by fluorescence spectroscopic techniques and ab initio density functional theory calculations with Becker's three-parameter Lee–Yang–Par (B3LYP) exchange functional with 6-311G basis set.

Graphical abstract

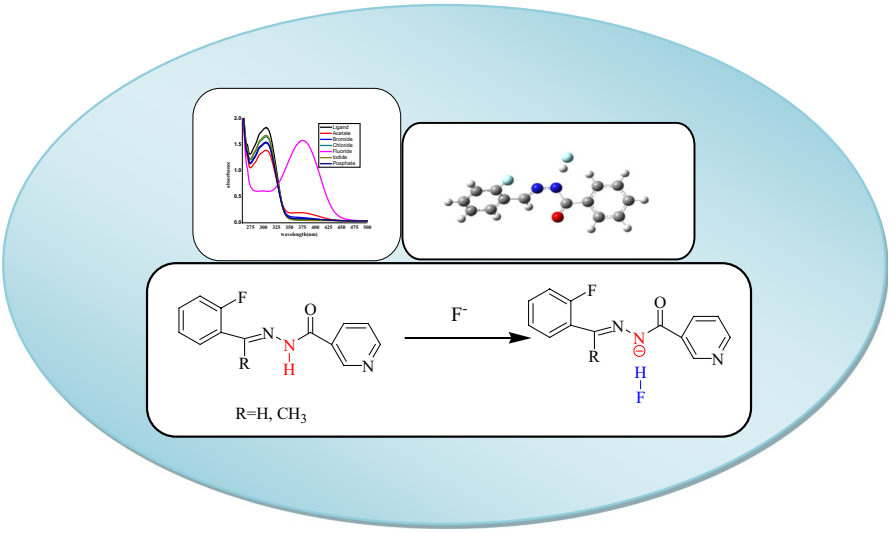

Keywords Acylhydrazones · TD-DFT · Ab initio · Fluoride sensing · Anion recognition

Published online: 03 October 2018

Introduction

We discuss the fluoride sensing ability of acylhydrazones *N*′-[1-(2-fluorophenyl) ethylidene]pyridine-3-carbohydrazide (**R1**) and *N*′-[2-fluorobenzylidene]benzohydrazide (**R2**) in acetonitrile. Optical and electrochemical sensing of biochemically and environmentally important species has emerged as a focus of attention for research into sensor design in the contemporary era [1–4]. In particular, the progress of fluoride ion chemosensors is of great importance, due to its advantageous impacts on human physiology [5, 6]. Among inorganic anions, the fluoride ion plays a special role in bone growth, tooth care, and related metabolic activities. Additionally, fluoride is an effective component in drugs and fabrication of nuclear weapons [7–9]. Although fluorine intake is fast, it is discharged slowly. Excess fluoride consumption results in acute fluorosis and is identified as one of the potential threats faced by many people living in India. Mining as well as other related activities result in unnatural concentrations of fluoride along with other anions. This subject is very important in the present environmental scenario too. Lessened rainfall and global warming will increase the atmospheric temperature, raising the concentration of fluoride ion in surface water. Being very small in size and highly electronegative, detection of fluoride in protic solvents when present in minute concentrations has always been a challenge, as has its removal. As a result of its significance, detection of fluoride using an effectively synthesized receptor and negligible instrumental help is greatly favored for effective applications. For this reason, colorimetric chemosensors have attracted immense interest in recent years [10–12].

Functional groups which have been explored as good receptors for fluoride ions include amides, pyrrole, urea/thiourea, imidazolium, phenylhydrazone, etc. [13–17]. However, the majority of these suffer from interference from other anions. Hydrazones are widely used in analytical chemistry as a selective metal-extracting agent, as well as in spectroscopic determination of certain transition metals. They have been the subject of extensive investigation due to their versatile chelating behavior, in particular those derived from pyridoxal phosphate and isonicotinic acid. Their potential hydrogen-donor ability also supports the sensing behavior of hydrazone compounds. In this connection, we synthesized two acylhydrazones and studied their fluoride sensing ability using experimental and theoretical approaches.

Results and discussion

The structural formula of compounds **R1**, **R2** is shown in Fig. 1.

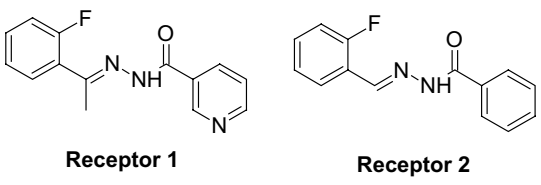

Fig. 1 Structural formula of receptors **R1**, **R2**

Good-quality crystals were separated from methanolic medium, and the crystal structures reported in *Acta E* [18–20]. Characteristic infrared (IR) stretching frequencies of imine-containing chelating groups in receptors **R1**, **R2** appeared at 1538 and 1558 cm^{-1}, respectively. The ^{1}H nuclear magnetic resonance (NMR) spectrum of *R1* showed two singlets at δ 10.95 and δ 2.36 ppm, attributed to N–H protons and methyl protons, respectively. For **R2**, subsequent NH protons appeared at δ 10.05 and singlet hydrogen at 9.03 ppm in the ^{1}H NMR spectrum.

Colorimetric analysis and UV–Vis spectral analysis

The interaction of receptors **R1**, **R2** with various anions such as fluoride, chloride, iodide, bromide, dihydrogen phosphate, and acetate ions was investigated in acetonitrile by colorimetric analysis. Appreciable color changes from colorless to yellow were observed for the receptors on addition of fluoride anion, while other anions failed to cause color changes. This inability to cause any significant color change in the receptor solutions indicates no recognition of these anions except fluoride. This is well supported by ultraviolet–visible (UV–Vis) analysis. The spectral profiles in Figs. 2 and 3 show absorption peaks at 281 and 293 nm, attributable to $\pi \rightarrow \pi^{*}$ transitions for **R1** and **R2**, respectively. Compounds **R1** and **R2** showed absorption at 308 and 306 nm, respectively, assigned to $n \rightarrow \pi^{*}$ transition. Significant variation in the absorption spectra was identified with fluoride ion, because of complexation between the host and guest molecules. Moreover, receptor **R2** exhibited a new peak for acetate ion with less

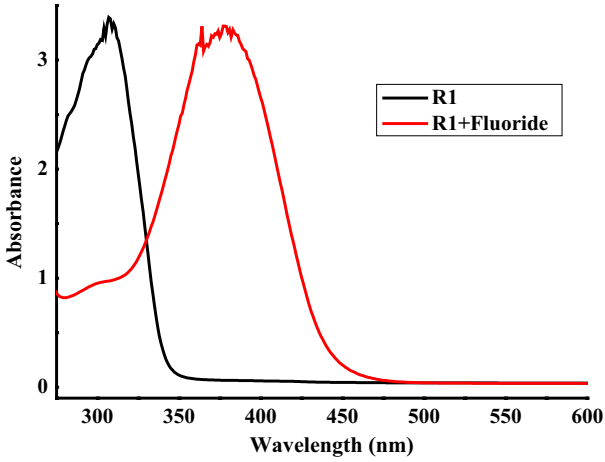

Fig. 2 Absorption spectra of *N*′-[(1*E*)-1-(2-fluorophenyl)ethylidene]pyridine-3-carbohydrazide (**R1**) with fluoride ion

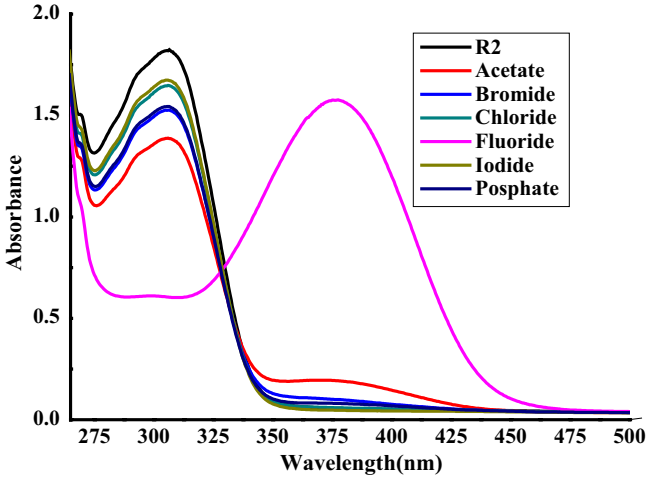

Fig. 3 Absorption spectra of *N*′-[(*E*)-2-fluorobenzylidene]benzohydrazide (**R2**) with different TBA anions

intensity at 375 nm. Slight variation in color was observed for *R2* when mixing with acetate too.

To determine the anion sensing ability of the compounds with fluoride and acetate at 298 K, titrations were carried out in acetonitrile and monitored using UV–Vis spectroscopy. The experiment was performed by preparing 5×10^{-5} mol L^{-1} solution of compounds **R1** and **R2** in acetonitrile, followed by addition of tetrabutylammonium ions at different concentrations. As the amount of fluoride ion in the UV–Vis titrations was increased, the receptors showed an intensity decrease and a

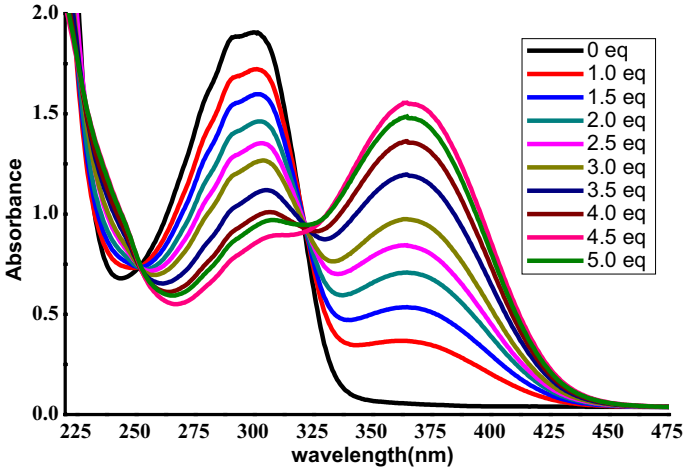

Fig. 4 Absorption spectra of *N*′-[(1*E*)-1-(2-fluorophenyl)ethylidene]pyridine-3-carbohydrazide (**R1**) [5×10^{-5} M] with different equivalents of fluoride ion

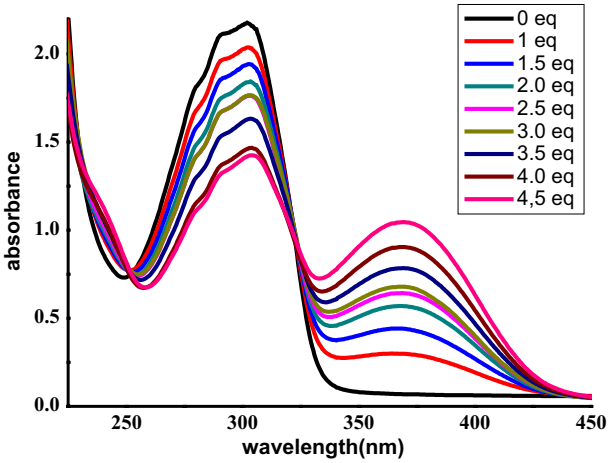

Fig. 5 Absorption spectra of *N*′-[(*E*)-2-fluorobenzylidene]benzohydrazide [5×10^{-5} M] (**R2**) with different equivalents of fluoride ion

small bathochromic shift in the absorption band corresponding to $n \rightarrow \pi^*$ transitions, plus subsequent formation of a new band at 368 and 377 nm, respectively. Both the new transition band and relative intensity of the receptor with respect to the band upon addition of fluoride depended on the receptor used, as shown in Figs. 4 and 5.

Fluorescence spectral studies

The fluorescence spectrum of both receptors **R1**, **R2** was monitored in acetonitrile. The excitation wavelength was optimized and chosen as 398 and 375 nm for **R1** and **R2**, respectively. When 0–5 equivalent of tetrabutylammonium fluoride was added to the solution of receptors **R1**, **R2**, a concomitant increase of the fluorescence intensity was observed. The fluorescence spectral profiles are shown in Figs. 6 and 7.

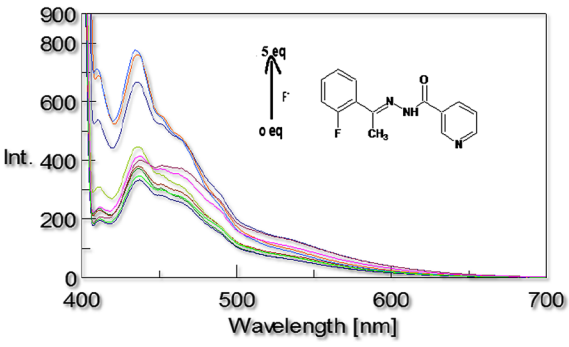

Fig. 6 Emission spectra of *N*′-[(1*E*)-1-(2-fluorophenyl) ethylidene]pyridine-3-carbohydrazide (**R1**, 100 μM) at 398 nm

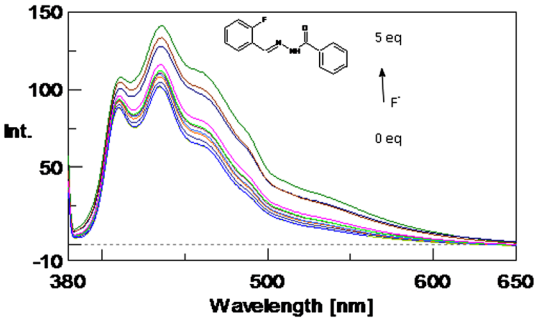

Fig. 7 Emission spectra of *N*′-[(*E*)-2-fluorobenzylidene] benzohydrazide (**R2**, 100 μM) in acetonitrile at 375 nm

Addition of fluoride anion induced a slight red-shifted emission band at 438 (**R1**) and 450 nm (**R2**). These are clear indications that the so-called fluorescence enhancement results from removal of the $n \rightarrow \pi^*$ transitions which normally mask the $\pi \rightarrow \pi^*$ transition that is mainly responsible for the emission behavior. Hence, the recognition of a molecule does not simply absorb color but also involves serious electronic reorganization within the molecule, appreciably affecting the highest occupied molecular orbital (HOMO) and lowest unoccupied molecular orbital (LUMO) interactions. In the same conditions, no significant spectral changes were observed on addition of 5 equivalents of other tetrabutylammonium anion salts.

Computational details

UV–Vis and fluorescence spectral studies confirmed selective sensing of fluoride ion by the receptors. To investigate the chemosensing mechanism of **R1**, **R2** toward F^- ions, computational calculations using ab initio density functional theory (DFT) for the structural properties of the receptors and their complexes with F^- ion were carried out. DFT calculations with Becker's three-parameter Lee–Yang–Par (B3LYP) exchange functional with 6-311G basis set were carried out for geometry optimization. The optimized ground-state structures of **R1**, **R2** and their fluoride complexes are shown in Fig. 8. The energy gap between the HOMO and LUMO molecular orbitals of **R1**, **R2**, and their fluoride complexes are shown in Fig. 9. The bond parameters of the optimized structures of the receptors are presented in Table 1. Selected experimental and theoretical parameters for **R1**, **R2** are presented in Table 2. The results show that the experimental and theoretical values are in good agreement with recent contributions in the field [18–22].

The N9–H19 and C10–O bond distances of **R1** in ground state were found to be 1.01 and 1.22 Å respectively, being increased in the **R1**–F complex. This bond length elongation can be ascribed to N9–H19 bond breakage and generation of a single bond between C10–O, while C7–N8 and N8–N9 had approximately equivalent values in **R1** and **R1**–F. The theoretical bond distances of N10–H and N10–C11 were 1.00 and 1.38 Å, respectively, for **R2**. The increase of these distances in **R2**–F can be attributed to bond elongation due to addition of fluorine. The shortening of the N8–N9 and N9–N10 bond distances after addition of fluorine also supports the sensing ability of the acylhydrazones. The calculated F–H values of **R1**–F and **R2**–F

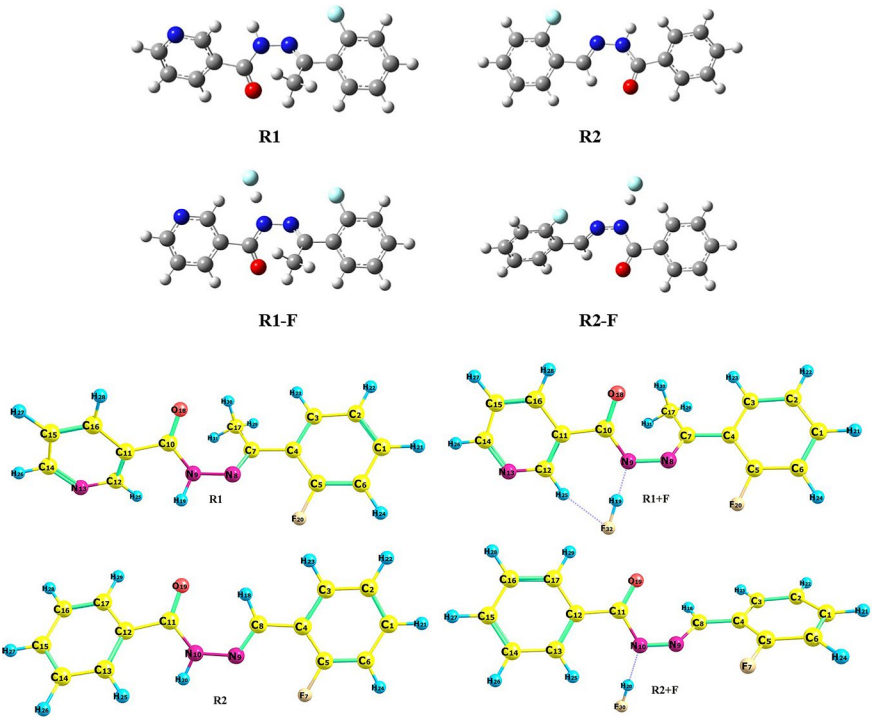

Fig. 8 Optimized ground-state geometry of **R1**, **R2**, **R1**–F, and **R2**–F

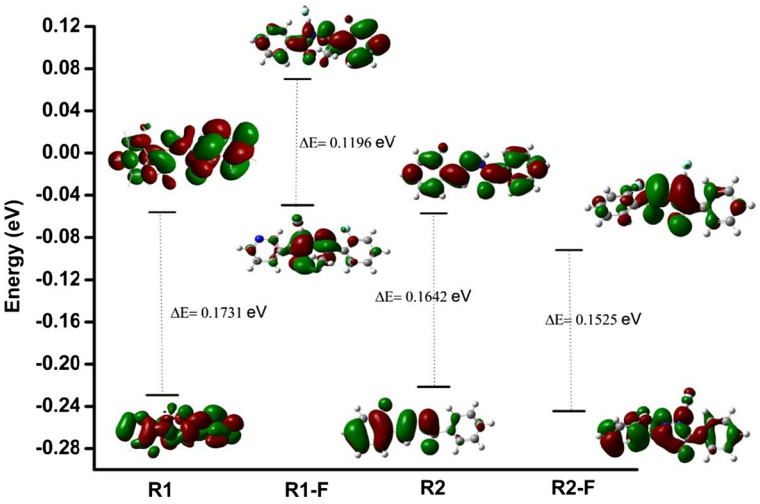

Fig. 9 Energy gap between HOMO and LUMO orbitals of **R1**, **R1**–F, **R2**, and **R2**–F

Table 1 Bond characters of **R1**, **R2**, **R1**–F, and **R2**–F at ground state

	R1	**R1**–F		**R2**	**R2**–F
C4–C7	1.48		C8–H12	1.08	1.09
C7–N8	1.28	1.29	C8–N9	1.29	1.28
N8–N9	1.39	1.37	N9–N10	1.37	1.29
N9–H19	1.01	1.35	N10–H	1.00	1.69
C10–O	1.22	1.25	N10–C11	1.380	1.43
C10–N9–N8	122.93	119.06	C11–O	1.22	1.22
N8–N9–C10–O	14.805	1.897	O–C11–N10–N9	2.37	17.45
F–H	–	1.02	F–H	–	0.96

were 1.02 and 0.96 Å, respectively, close to the value for a fluorine–hydrogen single bond. Therefore, a plausible mechanism for the addition of fluorine in **R1**, **R2** is shown in Fig. 10.

Conclusions

Two acylhydrazone receptors **R1**, **R2** were synthesized in good yield via condensation reaction. Both receptors **R1**, **R2** exhibited higher sensitive for fluoride anion with a prominent color change observable to the naked eye. They were found to provide anion recognition through H-bonding interactions. The sensing ability and binding affinity of both receptors towards fluoride were examined using spectroscopic techniques and ab initio DFT calculations, revealing high sensitivity for and selectivity towards fluoride even in a biologically competing solvent such as acetonitrile.

Experimental section

Materials and methods

2-Fluoroacetophenone, 2-fluorobenzaldehyde, nicotinic acid hydrazide, benzoic acid hydrazide (Fluka), and tetra-*n*-butylammonium salts (Aldrich) were of analytical grade and stored in vacuum desiccators containing self-indicating silica gel, being used without further purification. All solvents were purified prior to use.

^{1}H NMR spectra of the samples were recorded on a Bruker Avance 500 (500 MHz) spectrometer in $CDCl_3$ at 298 K with tetramethylsilane (TMS) as internal standard. FT-IR spectra were measured on a PerkinElmer FT-IR spectrometer using KBr pellets. UV–Vis and fluorescence spectra were recorded in 1-cm-path-length quartz cell on a PG Instrument T90+ spectrophotometer and JASCO FP-8300 spectrofluorophotometer, respectively.

Table 2 Selected experimental and theoretical parameters of **R1** and **R2**

R1				**R2**			
Bond parameter (Å, °)	Experimental	Computational	Difference	Bond parameter (Å, °)	Experimental	Computational	Difference
C4–C7	1.49	1.48	0.01	C4–C8	1.38	1.46	0.08
C7–N8	1.27	1.28	0.01	C8–N9	1.26	1.29	0.03
N8–N9	1.38	1.39	0.01	N9–N10	1.37	1.37	0
N7–C10	1.35	1.38	0.03	F–C5	1.34	1.34	0
N13–C12	1.33	1.33	0	C11–O	1.23	1.22	0.01
C–F	1.28	1.34	0.06	C11–C12	1.48	1.50	0.02
C10–O	1.22	1.22	0	C4–C8	1.38	1.46	0.08
N13–C14	1.34	1.33	0.01	C11–N10	1.33	1.38	0.05
F–C5–C4	120.6	120.38	0.22	O–C11–N10	121.02	123.65	2.63
C10–N9–N8	118.26	122.93	4.67	C8–N9–N10	116.26	120.29	4.03
C7–N9–N8	117.22	117.50	0.28	C11–N10–N9	118.79	131.15	12.36
C11–C10–N9	115.94	114.56	1.38	F–C5–C4	118.30	120.16	1.86
C14–N13–C12	115.8	117.25	1.45	F–C5–C6	117.84	117.51	0.33
C4–C7–N8	115.06	116.08	1.02	C4–C8–N9	119.94	121.63	1.69
O–C10–N9	123.50	123.60	0.1	N9–C8–H18	120.0	122.26	2.26
O–C10–C11	120.55	121.83	1.28	O–C11–C12	120.36	121.86	1.5
F–C5–C4–C7	3.5	2.24	1.26	F–C5–C6–C1	179.36	179.98	0.62
F–C5–C6–C1	177.3	178.57	1.27	C8–N9–N10–C11	2.89	3.25	0.36
C4–C7–N8–N9	178.48	177.52	0.96	F–C5–C4–C3	179.3	179.97	0.67

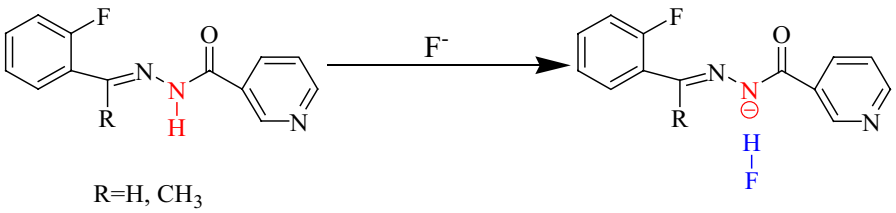

Fig. 10 Suggested mechanism of sensing

Synthesis of acylhydrazone compounds R1, R2

The receptors were prepared by adapting the reported procedure [23–25]. Methanolic dispersion of nicotinic acid hydrazide and benzoic acid hydrazide (0.137 g, 1 mmol) were added, respectively, with 2-fluoroacetophenone and 2-fluorobenzaldehyde (0.138 g, 1 mmol) in methanol. After addition of glacial acetic acid, the reaction mixture was refluxed for 6 h. The crystallized product was filtered off, washed with a minimum quantity of methanol, and dried over P_4O_{10} in vacuo. The receptors were characterized by IR and ^{1}H-NMR spectroscopy.

***N′*-[1-(2-Fluorophenyl)ethylidene]pyridine-3-carbohydrazide (R1)** Colorless, $C_{14}H_{12}FN_3O$, yield 80 %, melting point 166–168 °C. IR data (KBr, cm^{-1}): 3212, 3037, 2835, 1659, 1612, 1538, and 1494. ^{1}H NMR (400 MHz, $CDCl_3$, δ, ppm.): 10.95 (s, 1H), 7.26–8.03 (m, 8H), 2.36 (s, 3H).

***N′*-[2-Fluorobenzylidene]benzohydrazide (R2)** Colorless, $C_{13}H_{10}FN_3O$, yield 76 %, melting point 195–197 °C. IR (KBr, υ in cm^{-1}): 3216, 3069, 2835, 1642, 1614, 1558, 1493. ^{1}H NMR (400 MHz, $CDCl_3$, δ, ppm.): 10.05 (s, 1H), 7.26–8.00 (m, 9H), 9.03 (s, 1H).

UV–visible and fluorescence titrations

Stock solutions of **R1**, **R2** were prepared in acetonitrile. TBA salt (F^-, Cl^-, Br^-, I^-, ClO_4^-, $H_2PO_4^-$, and AcO^-) solutions were prepared at concentration of 1×10^{-5} mol L^{-1} in acetonitrile. Different equivalents of tetrabutylammonium salts (F^-, Cl^-, Br^-, I^-, ClO_4^-, $H_2PO_4^-$, and AcO^-) were added to the receptors, and their corresponding UV–visible and fluorescence spectra were recorded at 298 K.

Computational methods

All calculations were performed using Gaussian 09 software. Hybrid density functional theory (DFT) calculations were carried out using the B3LYP method with 6-31G+(*d*, *p*) basis set to optimize the ground-state geometry of the receptors and receptor–fluoride complexes [26, 27]. The 6-31G(*d*, *p*) basis set is moderate and suitable for such large organic compounds, being a proper basis set for ionic compounds. To investigate the solvent effect of dimethylsulfoxide (DMSO, dielectric

constant 46.826), polarized continuum model (PCM) calculations were performed throughout the steps.

Acknowledgements P.B.S. is grateful for financial support from CHRIST (Deemed to be University), Bengaluru.

References

1. Y. Zhou, Z. Xu, J. Yoon, Chem. Soc. Rev. **40**, 2222 (2011)
2. H.N. Kim, W.X. Ren, J.S. Kim, J. Yoon, Chem. Soc. Rev. **41**, 3210 (2012)
3. Y. Zhou, J. Yoon, Chem. Soc. Rev. **41**, 52 (2012)
4. J. Jose, R. Datta, P.B. Sreeja, Orient. J. Chem. **33**, 1438 (2017)
5. H.T. Chifotides, B.L. Schottel, K.R. Dunbar, Acc. Chem. Res. **46**, 894 (2013)
6. V. Baelum, S. Pongpaisal, W. Pithpornchaiyakul, S. Pisuithanakan, R. Teanpaisan, P.N. Papapanou, G. Dahlen, O. Fejerskov, Acta Odontol. Scand. **60**, 80 (2002)
7. S. Purser, P.R. Moore, D.O. Hagan, S. Purser, P.R. Moore, Chem. Soc. Rev. **37**, 320 (2008)
8. A. Strunecka, P. Connett, J. Appl. Biomed. **2**, 141 (2004)
9. H. Rosenberg, J.C. Mosteller, W. Air, W.A.F. Base, O.F.W. Spray, Ind. Eng. Chem. **45**, 2283 (1953)
10. Z. Liang, W. Limin, Z. Guanjun, Y. Jianjun, C. Xiaofei, T. Mingshuang, W. Yue, Chin. J. Chem. **30**, 2823 (2012)
11. Y. Qu, J. Hua, H. Tian, Chem. Soc. Rev. **39**, 3007 (2010)
12. D.A. Jose, D.K. Kumar, B. Ganguly, A. Das, Org. Lett. **6**, 3445 (2004)
13. P.D. Beer, P.A. Gale, Angew. Chem. Int. Ed. **40**, 486 (2001)
14. P.A. Gale, Coordin. Chem. Rev. **240**, 191 (2003)
15. V. Amendola, D. Esteban-go, Ä. Mez, L. Fabbrizzi, M. Licchelli, C. Generale, Acc. Chem. Res. **39**, 343 (2006)
16. P.A. Gale, R. Quesada, Coord. Chem. Rev. **250**, 3219 (2006)
17. V.K. Gupta, R.N. Goyal, R.A. Sharma, Talanta **76**, 859 (2008)
18. P.B. Sreeja, M. Sithambaresan, N. Aiswarya, M.R.P. Kurup, Acta Crystallogr. E **70**, o115 (2014)
19. P.B. Sreeja, M. Sithambaresan, N. Aiswarya, M.R.P. Kurup, Acta Crystallogr. E **70**, o532 (2014)
20. P.B. Sreeja, M. Sithambaresan, N. Aiswarya, M.R.P. Kurup, Acta Crystallogr. E **69**, o1828 (2013)
21. A. Saeed, S. Ashraf, J.M. White, D.B. Soria, C.A. Franca, M.F. Erben, Spectrochim. Acta Part A **150**, 409 (2015)
22. I. Arshad, J. Yameen, A. Saeed, J. White, F. Albericio, Crystals **7**, 19 (2017)
23. P.B. Sreeja, A. Sreekanth, C.R. Nayar, M.R.P. Kurup, A. Usman, I.A. Razak, S. Chantrapromma, H.K. Fun, J. Mol. Struct. **645**, 221 (2003)
24. P.B. Sreeja, M.R.P. Kurup, A. Kishore, C. Jasmin, Polyhedron **23**, 575 (2004)
25. P.B. Sreeja, M.R.P. Kurup, Spectrochim. Acta Part A **61**, 331 (2005)
26. T. Yanai, D.P. Tew, N.C. Handy, Chem. Phys. Lett. **393**, 51 (2008)
27. I. Yilmaz, A. Cukurovali, Dyes Pigm. **83**, 211 (2009)

Affiliations

Jemini Jose[1] · A. Sreekanth[2] · Athira M. John[1] · Sabeel M. Basheer[2] · P. B. Sreeja[1]

✉ P. B. Sreeja
sreeja.pb@christuniversity.in

[1] Department of Chemistry, CHRIST (Deemed to be University), Hosur Road, Bangalore 560029, India

[2] Department of Chemistry, National Institute of Technology, Tiruchirappalli 620015, India